Swarming Driftcams: a Novel Platform for Locating and Tracking Pelagic Scattering Layers

Eric J. Berkenpas[1], Charles M. Shepard[1], Rachel Suitor[2], Paul Zaidins[2], Derek Paley[2], and Kyler Abernathy[3]

[1]*Second Star Robotics, Silver Spring, MD USA;* [2]*University of Maryland, College Park, MD, USA;* [3]*National Geographic Society, Washington, DC, USA*

***Abstract*— This paper presents the design, development, and field results of novel depth-controlled sensor platforms. Called the "Swarming Driftcams," these platforms travel passively in horizontal direction with ocean currents while controlling and profiling depth. These platforms use integrated depth, acceleration, attitude, temperature, and camera sensors to collect data from water column ecosystems. A novel buoyancy engine, using an electrically actuated reciprocating pump, facilitates active depth correction to a maximum depth of 700 m. Embedded computers control data collection, camera, lighting, and depth control. The vehicle contains a combination USBL and acoustic modem for bidirectional communication and surface tracking as well as intervehicle communications. A radio beacon and an Iridium GPS satellite beacon aid in surface location and recovery. In addition, the system has a small form factor, measuring 1 m in total height with a mass of 48 kg. Multiple vehicles can be deployed and tracked enabling increased data collection and the possibility for cooperative sampling strategies within the water column. All aspects of the vehicle hardware are discussed. Preliminary results are also presented for recent deployments into scattering layers in the Gulf of Mexico.**

Index terms*— *swarm, floats, imaging, Lagrangian, scattering layers, buoyancy control

I. Introduction

Pelagic ecosystems (also called scattering layer ecosystems) are the largest living communities on Earth containing swimming fishes, crustaceans, cephalopods, and gelatinous organisms collectively known as micronekton [1]. These organisms inhabit an important position within oceanic food webs between phytoplankton and apex predators. Micronekton form dense aggregations which migrate to the surface during the evening returning to depth during the day. These migrations are thought to be critical to the ocean's means of absorbing atmospheric carbon [2].

Studying scattering layers is often carried out using a combination of ship-based echosounder surveys, in-situ chemical sensing, net sampling, and genetic analysis [3]. These methods are highly effected for making large-scale surveys but lack the ability to collect fine-scale behavioral information. Net sampling is thought to be somewhat problematic since it can remove significant biomass from the area under study. Camera-based in-situ solutions can significantly improve researchers' understanding of animal behavior and food webs within scattering layer ecosystems while being minimally invasive.

Techniques for collecting in-situ imagery of these animals beyond 50 m depth typically use manned submersibles [4] – [6], remotely operated vehicles [6] – [9] or autonomous underwater vehicles [10]-[11]. The high-cost of these sampling methods limits the frequency that these techniques can be employed.

Lagrangian floats are robotic instruments often used to profile ocean chemical properties, typically conductivity, temperature, and dissolved oxygen with respect to depth [12]-[14]. By simultaneously deploying multiple low-cost camera-based sensors into pelagic scattering layer ecosystems, a large amount of in-situ behavioral data can be collected. Building upon a previous prototype hardware platform [15] - [16], a novel system employing multiple tetherless, depth-controlled vehicles operating simultaneously has been developed and tested to collect in-situ fine-scale mesopelagic data and video (Fig. 1). These vehicles are called Driftcams and utilize acoustic communications, tracking, and real-time ship-based and vehicle-based sensing to insert cameras into the depths inhabited by micronekton.

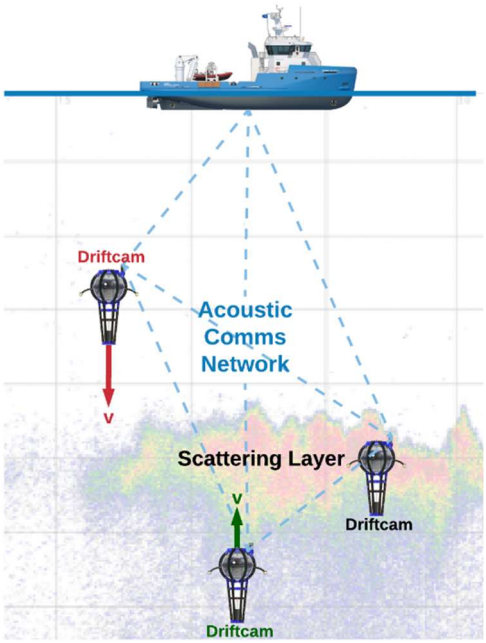

Fig. 1. The swarming Driftcam concept utilizes multiple vehicles deployed from a surface platform, simultaneously sampling scattering layer ecosystems with camera-based sensors.

This work was supported by the National Geographic Society and a grant from the National Oceanic and Atmospheric Administration, Office of Ocean Exploration (NA18OAR0110290).

II. Theory and System Design

The Driftcam was developed to tetherlessly image migrating pelagic scattering layers through a combination of camera sensing and precision buoyancy control. The vehicle was designed to be small, low-cost, and easy to deploy from vessels of opportunity.

The Driftcam vehicles use a pump-based buoyancy engine to control vertical motion and depth. The motion of a buoyancy controlled underwater vehicle can be described by the following equation of motion:

$$M\dot{v} + C(v)v + D(v)v + g(\eta) = \tau \quad (1)$$

Where v, is the body-fixed velocity and rate-rotation vector, and $\dot{v}$ is the body-fixed acceleration vector, M is the inertial matrix, $C(v)$ is the coriolis-centripetal matrix, $D(v)$ is the damping matrix, $g(\eta)$ is the restoring force vector and τ is a vector of input forces to the system. A full treatment of (1) can be found in [17].

For the purposes of a depth-controlled vehicle drifting passively with ocean currents we can neglect rotation and horizontal motion. The velocity vector can be reduced to a scalar w which is the component of velocity in the vertical direction. In the vertical direction the system's inertial matrix reduces to

$$M = m + Z\dot{w} \, . \quad (2)$$

Where m is the vehicle's mass and $Z\dot{w}$ the added mass parameter in the vertical direction. The coriolis-centripetal matrix reduces to zero because the system is irrotational.

The dampening matrix reduces to

$$D(v) = Z_w|w| + Z_w w|w| \, . \quad (3)$$

Where Zw and $Z_w w$ are dampening parameters in the vertical direction.

The restoring force vector $g(\eta)$ reduces to

$$g(\eta) = B - W \, . \quad (4)$$

The force of buoyancy B and the system weight W are given by the following:

$$B = \rho a_g V \quad (5)$$

$$W = a_g m \, . \quad (6)$$

Where ρ is the density of displaced seawater and a_g is the acceleration due to gravity. The vehicle volume, V, is given by

$$V = V_{static} + V_{eng} . \quad (7)$$

Where V_{static} is the minimum volume of the vehicle and V_{eng} is volume added by the buoyancy engine. The force in the vertical direction, Z, can therefore be expressed as follows:

$$wm + wZ_{\dot{w}} + wZ_w|w| + wZ_w|w|w + \rho a_g(V_{static} + V_{eng}) - a_g m = Z \, . \quad (8)$$

Applying initial conditions, the resulting equation of motion can be used to calculate acceleration, velocity, and position over time and was implemented as part of a simulation in MATLAB (The MathWorks Inc.) using Euler's method. The simulated model was used to estimate the energy requirements of the system and the necessary size and precision of the buoyancy engine pump.

Using depth feedback, a controller was implemented to command engine volume thus control depth. This controller is described in previous work by the authors [16]. Numerical simulation was also used to test and tune the depth control algorithm.

A drawing of a Driftcam vehicle is shown in Fig.2. A glass spherical housing contains the buoyancy engine, control computer, battery system, and camera. A second cylindrical housing holds a USBL system (Seatrac X150, Blueprint Subsea). The USBL system contains the main sensors used to allow the Driftcam to communicate, be tracked, and determine its depth and location. Because of the sensitivity of these sensors to electrical and magnetic field fluctuations it was decided to house them separately.

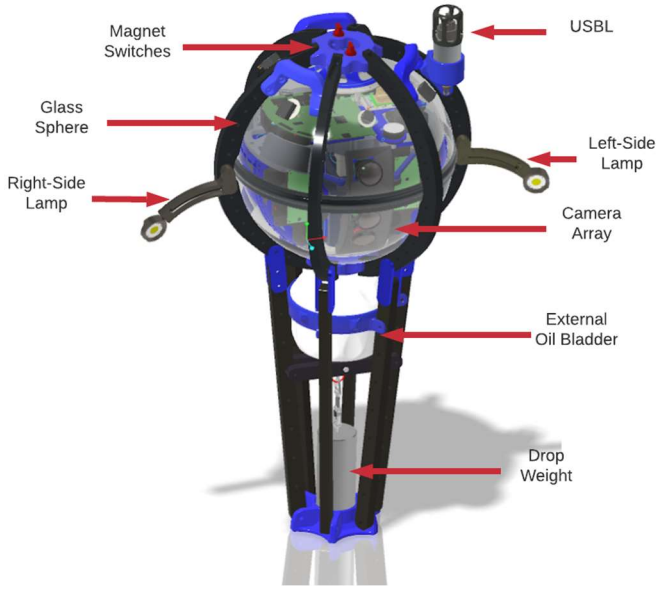

Fig. 2. A drawing of a Driftcam vehicle showing the glass sphere, lamps, external bladder, camera array, and USBL system. Total height of the platform is 1 m.

The buoyancy engine consists of an electrically actuated reciprocating hydraulic pump which moves inert mineral oil into an external expandable volume. For actuation, a 1.9 N-m NEMA 23 stepper motor is coupled to a crankshaft via a steel belt providing to drive a 0.85 mL piston. A pair of electronically actuated solenoid valves control the direction of fluid flow as the pump actuates. A single count-per-revolution indexing encoder is used to calibrate valve timing and a 1000 count-per-revolution high-resolution encoder is used to estimate fluid flow and total volume pumped for control feedback purposes. The buoyancy engine allows up to 2 L of added adjustable volume to the vehicle at a maximum flow rate of 0.76 mL/s. The engine is designed to operate at up to 700 m depth and actuate against 7 MPa of ambient pressure and hold against at least 20 MPa. The maximum depth is limited by rating of the valves.

An electrical block diagram of the Driftcam system is provided in Fig. 3. The electrical design is comprised of a main controller board which controls the camera, communications,

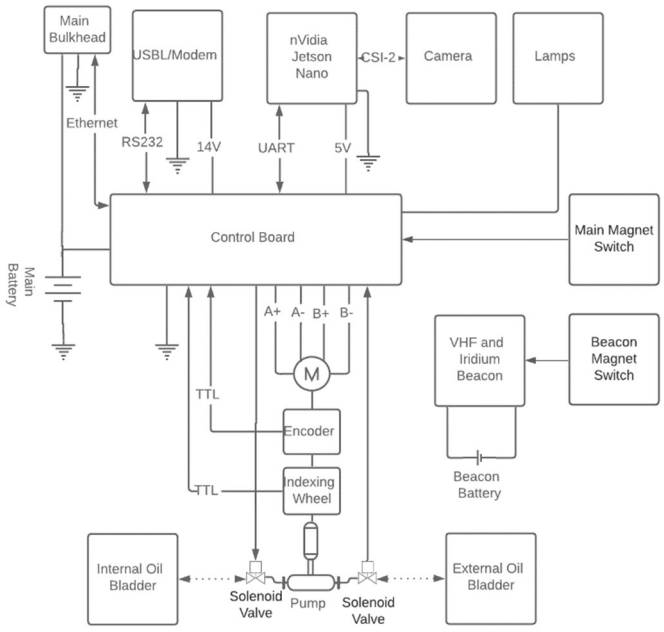

Fig. 3. An electrical block diagram showing the control board, bulkhead connections, buoyancy engine, embedded Linux computer, USBL, VHF/Iridium beacon, and lamps. Additionally, the fluidic system of the buoyancy engine is show with the pump, valves, and internal and external bladders.

sensors, buoyancy engine, and lamps. A 10-cell, 36 V nominal, 936 W-hr battery provides power to the vehicle. The indexing encoder and high-resolution encoder connect to a 16-bit microcontroller (PIC24, Microchip Technology) running the depth controller. A main electrical bulkhead connector through the glass sphere provides facility for battery charging and programming. An ethernet connection allows video and data to be downloaded.

An embedded computer running the Linux operating system (Tegra X1, nVidia Corporation) provides video recorder capabilities. This platform provides hardware h.264 encoding as well as a highly-parallel GPU architecture allowing complex image processing in real-time using the open computer vision library (OpenCV). A camera is connected to the embedded computer via a CSI-2 interface.

In typical use the buoyancy engine is expected to be the primary method by which the vehicle will return to the surface when its mission is complete. A backup system consisting of a 7 kg drop weight, burn-wire, and a galvanic time release (GTR, Neptune Marine Supply) has been incorporated in the event of buoyancy engine failure or rapid recovery is needed. A nylon-coated, stainless-steel burn-wire is electrically connected to the controller via the main electrical bulkhead. When current is passed through the wire, it rapidly corrodes at an exposed metal point through electrolytic erosion and releases a drop-weight, allowing the Driftcam to ascend to the surface. The GTR acts as a further back-up release in the case of burn-wire failure. It is a passive device that begins corroding once exposed to salt water, and takes between 12 and 36 hrs to release, depending on temperature, current, and salinity.

The controller also commands the main lighting system to strobe at regular intervals to provide a visible indicator when on the surface after dark, and an orange flag is used during daylight operations.

Once on the surface, a 150 MHz VHF transmitter (Telonics, MK8) allows the Driftcam to be located when using a directional antenna and receiver. An additional Iridium-based satellite beacon is used to provide global tracking via the Iridium satellite network (MetOcean, iBCN-BB). These beacons are enabled with a dedicated magnet switch. The beacon battery and system are electrically isolated from other system components to avoid system failures cascading to the beacon subsystem.

Video was recorded to solid state storage using GStreamer, an open-source multimedia framework for processing video, running on the embedded Linux computer. Video was saved as 1920x1080 frames at 30 frames per second using h.264 compression at an average rate of 30 Mb/s. Video data is saved to UTC-0 timestamped mpeg4 container files resident on the solid-state storage device for later download.

Because of the available computational power in the embedded Linux computer, the Driftcam has facility to perform real-time image processing with OpenCV. One proposed application of real-time image processing is to use the number of marine organisms at a specific depth captured by the onboard camera as a proxy for the distance to the center of a scattering layer. It is thought that the greatest concentration of swimming organisms should be at the center of the scattering layer and in general the count should taper off gradually with distance.

Two algorithms are proposed to attempt to measure real-time organism (or target) count ‘Blob Detection’ and ‘Farneback Optical Flow’. The first method, ‘blob detection’, is implemented in OpenCV. By subtracting a rolling mean frame and searching for blobs of pixels, that meet select criteria, a rough target count could be established. The second proposed method additionally would use the ‘Farneback Optical Flow’ algorithm as implemented by the OpenCV. This allows blobs to be further narrowed down to only those that are moving above a certain frame to frame speed allowing marine snow to be filtered from moving organisms. Preliminary testing with both algorithms with previously collected pelagic video data shows some promise for camera-based layer detection.

If equipped with real-time on-board image processing algorithms, each Driftcam can translate in situ optical data into meaningful sensor measurements for output-feedback calculations. Real-time image processing allows for continuous estimation of the scattering layer’s nominal depth, which is sampled intermittently by a reference-tracking controller [18]. The stability of the reference-tracking control is established by [18] for continuous- and discrete-time output-feedback. The reference-tracking controller takes in the aggregate data telemetered by the Driftcam and outputs a desired depth setpoint. Computations for the reference-tracking control can be run separately on a surface tender, outside of the Driftcam’s closed-loop depth control, without affecting the controller performance due to the slow-moving dynamics of the scattering layer. Implementing the high-level reference-tracking controller on the Driftcam’s embedded Linux computer would make fully autonomous operation possible.

Given the capabilities of an individual Driftcam, swarming strategies could be developed for the collective control of multiple Driftcam vehicles. One of the simplest swarming strategies is known as leader-follower (LF) control, in which a leader agent is commanded to the calculated desired depth setpoint and follower agents receive the leader's actual depth as their desired setpoint. The followers can either be sent to exactly where the leader is, for investigating a specific depth, or their commands can include a prescribed offset that allows the swarm to maintain relative vertical position between agents. It is preferable for the Driftcam swarm to maintain a separation between agents, so as to maximize the coverage area for simultaneous imaging of scattering layers. LF control is scalable to any number of vehicles and can be implemented most easily with a virtual leader. A virtual leader allows for all of the physical vehicles to be followers and all have identical control architecture. For larger numbers of vehicles, the desired separation between agents is computed with a weighted consensus control algorithm and relies only on local sensing information, making the swarm control more distributed. Using the acoustic communications network, each Driftcam can receive telemetry from its neighbors and use that data together with the leader's position to determine the separation parameter for its next setpoint. One major benefit of this inter-agent communication is that the swarm could regulate the inter-agent separations more often than it receives new setpoints from a surface vessel.

Currently there is also ongoing work into investigating new control strategies to allow the Driftcam agents to regulate their relative horizontal separation by taking advantage of the velocity-depth profile of the horizontal current.

III. Methods

Vehicle hardware and software has been tested via numerical simulation, hardware-in-the-loop simulation, pool testing, and finally sea-trials in the Gulf of Mexico (GoM).

Simulation was used as a tool for system identification. By using data collected from previous prototype Driftcam deployments [15] – [16], simulation was applied to search and refine added mass and dampening parameters. Parameters were estimated by fitting actual recorded depth tracks to simulations using the MATLAB *fminsearch* optimization function. Simulation parameters as well as fitted added mass and dampening parameters (bold) are indicated in Table I. Simulation was also used to search for stable control parameters.

TABLE I. SIMULATION PARAMETERS

SYMBOL	DESCRIPTION	VALUE/UNITS
m	Mass of the system	48 kg
V_{static}	Static system volume	45.74 L
V_{eng}	Buoyancy engine added volume	0-2 L
ρ	Nominal Density of Seawater	1020 - 1025 kg m^{-3}
G	Gravitational Acceleration	9.8 m s^{-1}
$\boldsymbol{Z_{\dot{w}}}$	**Added Mass Parameter**	**-0.201 kg**
$\boldsymbol{Z_w}$	**Dampening Parameter**	**-3.847 kg s^{-1}**
$\boldsymbol{Z_{w\|w\|}}$	**Dampening Parameter**	**-104.229 kg m^{-1}**

Model parameters were then used to simulate vehicle motion using a hardware-in-the-loop (HIL) test setup (Fig. 4). This allowed the software, control system, power system, and buoyancy engine to be exercised in a real-time simulation. A personal computer running the MATLAB simulation provided sensor feedback by generating and sending USBL sensor messages to the Driftcam controller via an RS-232 connection. A DC power supply was used in place of the battery. The weight of the external bladder was measured on a digital scale to estimate volume displaced. These measurements were sent to the simulation computer via another RS-232 connection and were used to calculate system dynamics and update the simulated vehicle depth in real-time.

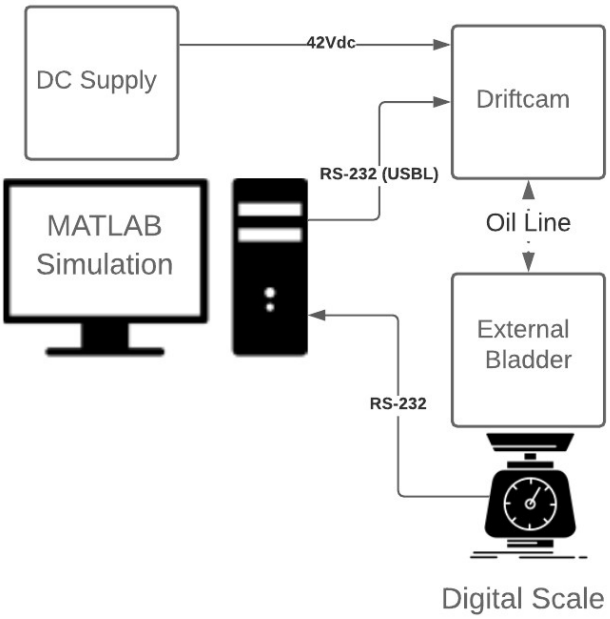

Fig. 4. A block diagram of the HIL test setup used to test vehicle control hardware. The test setup incorporates the Driftcam hardware including the external bladder, a digital scale, a DC supply, and a computer running a MATLAB simulation of vehicle dynamics.

Driftcams were deployed in a test pool at the University of Maryland, Space Systems Laboratory (SSL) Neutral Buoyancy Test Facility to exercise hardware and software in a simulated ocean environment. SSL contains a circular 15 m diameter 7.5 m deep freshwater pool and provided an environment to test hardware and software in-water. Typical tests were 1-hr deployments to depth setpoints 1-4 m. Tests were performed to validated model parameters, control parameters, acoustic communications, and mission plans in a controlled ocean-like environment. The facility also allowed accurate measurements of vehicle densities.

Ocean tests were performed from the R/V Point Sur in late July 2021, in the GoM approximately 150 km south of the Mississippi coast near 28° N and 87° W within the DEEPEND survey area [3]. Deployments occurred during glider, conductivity temperature and depth (CTD) profiling operations and echosounder surveys. Tests were performed individually and concurrently with one or two Driftcam vehicles. Before deployment, vehicles were ballasted for the local seawater density. Typically, vehicles were preprogrammed to dive to a depth of 100 m and then return to the surface after 2 hrs either via action of the buoyancy engine or by releasing the drop weight. After the Driftcams were observed to dive, tracking and communications were established via the USBL system. For

tracking, the ship's GPS NMEA strings were transmitted via an RS-232 connection to a personal computer running mapping software provided by the USBL manufacturer (Seatrac PinPoint, BluePrint Subsea). Acoustic messages were sent to the Driftcam by encoding them into as message payload within the USBL acoustic datagram using a MATLAB script. Responses were automatically decoded by the script and displayed to the terminal screen.

During deployments the ship's position was adjusted to to remain within 800 m of the Driftcam vehicles. The end-of-mission time and depth setpoint of the Driftcams were periodically adjusted to allow the vehicles to operate within scattering layers identified via the ship-based echosounder. The first four deployments were performed with individual vehicles to test communications, tracking, recovery, and camera functionality. Two additional deployments were performed by simultaneously releasing two Driftcams to test multiple vehicle deployments. Dives were performed at multiple times throughout the day and night to observe migrating scattering layers at depth and near the surface.

IV. Results and Discussion

Results of a representative SSL pool test are shown in Fig. 5. The pool presented a poor acoustic channel likely because of reverberation, multipath, and ambient noise due to the filtration system. Communication with a topside USBL transponder was achieved with occasional repositioning of the transducer. A small amount of trapped air in the external frame and bladder of the Driftcam is unavoidable. Expanding air volumes will produce a natural instability near the surface and therefore depth control within the relatively shallow pool is thought to be a worst-case environment for validating the control stability. Despite these limitations, the buoyancy engine was able to successfully control depth of the vehicle to within 1 m in the pool using the control parameters identified by simulation. During pool testing the buoyancy engine was observed to run around 90% of the time likely due to the instability caused by trapped air within the system.

A representative result of open-ocean testing is shown in Fig. 6. Two Driftcam vehicles were successfully deployed, tracked, and recovered a combine 8 times with 2 deployments occurring simultaneously. Vehicles collected both ambient and artificially illuminated video data from depths up to 454 m. Driftcams successfully adjusted their ballast and descended to preprogrammed setpoints and updated depths via acoustic surface commands.

USBL communications and tracking were successfully achieved at a range of 1.2 km although message transmission and tracking was significantly degraded at this range. Effective horizontal range was found to be about 750 m or less, with most messages transmitted receiving a response. Effective communication and tracking were also observed to be significantly better when Driftcams were at depths greater than 50 m. The platforms were able to effectively control depth at sea using control parameters identified by numerical simulation and validated in pool testing. Fig. 6c shows the representative depth track of two Driftcams deployed simultaneously. After diving at around 18 cm/s to preprogrammed depth setpoints of 100 m,

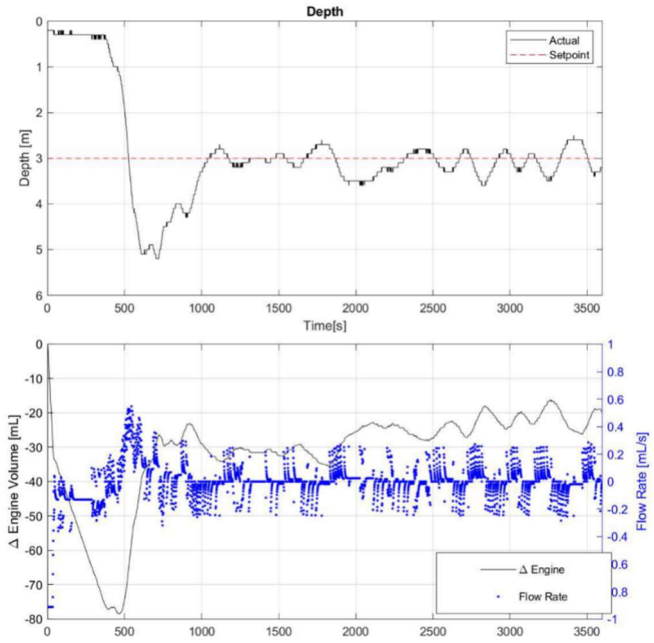

Fig. 5. Depth control results from a pool test indicating the Driftcam tracking a 3 m depth setpoint (top) and action of the buoyancy engine to correct vehicle density (bottom).

vehicles were commanded to go to other depths opportunistically in roughly 10 min increments. After settling on its 100 m setpoint, Vehicle 1 was commanded to go to 127.7 m, 162 m, 233.7 m, 314 m, 394 m, and 300 m before being commanded to return to the surface after a 2 hrs 40 min dive. From 100 m, Vehicle 2 was commanded to go to 127.7 m, 162 m, 217.6 m, 230.4 m, 262 m, and 321.7 m before being commanded to return to the surface after a 1 hr 51 min dive. Driftcams generally translated vertically to setpoint depths at around 15-20 cm/s. Significant overshoot was observed (40 – 50 m in some cases) however vehicles tended to settle on their setpoints within about 15 minutes to within 0.3 m absolute depth error. During dives, the buoyancy engine actuated 70-75% of the time.

Because seawater density generally increases with depth while vehicle density remains relatively constant, volume-based depth control is naturally stable with only minimal corrections in engine volume needed to adjust for local seawater density variations and thermal expansion of the vehicle. The somewhat continuous buoyancy engine actuation as observed in recent ocean tests, is not ideal since it uses the limited available energy and generates acoustic noise potentially affecting wildlife. Since control parameters were conservatively selected, based on rough estimates for drag and added mass from a larger prototype vehicle [16], significant improvements in control accuracy, stability, and efficiency can be obtained by modeling the new vehicle using data collected on this most recent cruise. Despite not being optimally tuned, Driftcams collected significant amounts of video data within and around acoustically identified scattering layers.

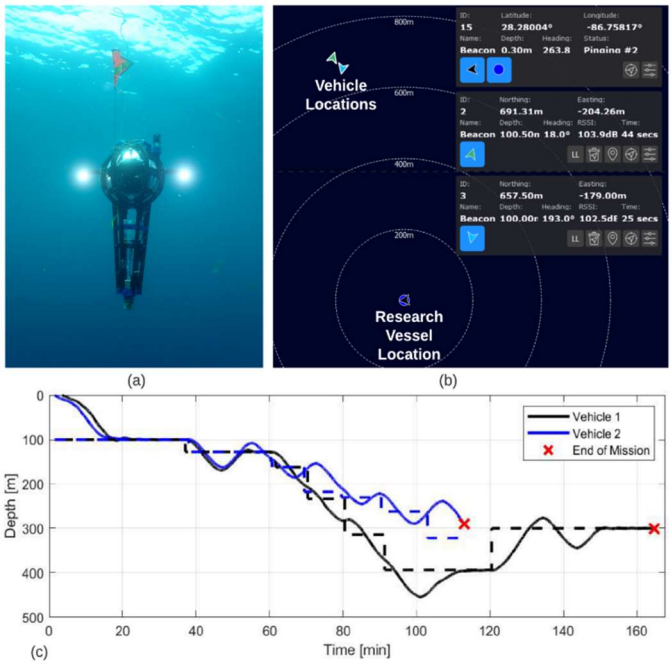

Fig. 6. Results of sea trials showing (a) a photo of a Driftcam descending from the surface towards its target depth, (b) an image of the mapping software used to track Driftcams during deployments indicating the location of two platforms, and (c) a simultaneous depth track of two vehicles during a deployment in the Gulf of Mexico. The solid line indicates the depth track and the dashed line indicates the setpoint.

V. Conclusions

Multiple small, acoustically-connected, tetherless drifting vehicles have been developed and fabricated. The Driftcams have been successfully deployed and recovered 8 times in open-ocean tests to depths up to 454 m in the Gulf of Mexico. The platforms were successfully controlled and tracked via an acoustic connection to a range of up to 1.2 km. Deploying, controlling, and tracking multiple Driftcam vehicles simultaneously has also been demonstrated. Dives occurred during simultaneous glider, CTD, and echosounder operations indicating the ability to deploy the system from vessels of opportunity. When used in conjunction with a scientific echosounder, vehicles were successfully directed to depths containing scattering layer aggregations to successfully collect video of micronekton. Data collected during dives showed the functionality of the camera, depth control, and recovery systems proving the utility of the Driftcam as a platform for surveying the mesopelagic zone.

Future work will involve improved modeling and simulation of the dynamics of Driftcam vehicles based on newly collected open-ocean data. Using improved simulation, we will optimize tuning the depth control system to improve accuracy, speed, and efficiency. The new video dataset will be used to create target detection algorithms which can be applied to swarming strategies such as LF towards a fully autonomous swarm.

Acknowledgment

The authors would like to thank D. Akin of the University of Maryland's Space Systems Laboratory, College Park, MD, USA, who provided facilities for pool testing. Additionally, the authors would like to thank M. Ahmed and A. Clarke who lent their skill and expertise towards assisting in fabrication of the many hardware components. Lastly, we would like to thank K. Boswell, C. Taylor, J. Horne, and the crew of the R/V Point Sur for their support and advice during the open-ocean testing in the Gulf of Mexico.

References

[1] S. Tont, "Deep scattering layers: Patterns in the pacific," California Cooperative Ocean Fish Investigation Rep., vol. 18, pp. 112–117, 1976.

[2] K. Hidaka, K. Kawaguchi, M. Murakami, and M. Takahashi, "Downward transport of organic carbon by diel migratory micronekton in the western equatorial Pacific: Its quantitative and qualitative importance," Deep Sea Res. I, Oceanogr. Res. Papers, vol. 48, no. 8, pp. 1923–1939, 2001, doi: 10.1016/S0967-0637(01)00003-6.

[3] A. Cook, A. Bernard, K. Boswell, H. Bracken-Grissom, M. D'Elia, and S. de Rada, et. al. "A Multidisciplinary approach to investigate deep-pelagic ecosystem dynamics in the Gulf of Mexico following Deepwater Horizon." Frontiers in Marine Science no. 7, 2020, doi: 10.3389/fmars.2020.548880.

[4] W. Kohnen, "Review of deep ocean manned submersible activity in 2013,"Marine Technol. Society J., vol. 47, no. 5, pp. 56–68, 2013. [Online]. Available: https://doi.org/10.4031/MTSJ.47.5.6

[5] Barham, "Deep scattering layer migration and composition: Observations from a diving saucer," Science, vol. 151, no. 3716, pp. 1399–1403, 1966, doi: 10.1126/science.151.3716.1399.

[6] B. Robison, "Deep pelagic biology," J. Exp. Marine Biol. Ecol., vol. 300, pp. 253–272, 2004, doi: 10.1016/j.jembe.2004.01.012.

[7] R. Capocci, G. Dooly, E. Omerdic, J. Coleman, T. Newe, and D. Toal, "Inspection-class remotely operated vehicles—A review," J. Marine Sci. Eng., vol. 5, no. 1, pp. 1–32, 2017, doi: 10.3390/jmse5010013.

[8] R. Christ and R Wernli, The ROV Manual: A User Guide for Remotely Operated Vehicles. Waltham, MA, USA: Elsevier, 2014.

[9] K. Raskoff, R. Hopcroft, K. Kosobokova, J. Purcell, and M. Youngbluth, "Jellies under ice: ROV observations from the Arctic 2005 hidden ocean expedition," Deep Sea Res. II, Topical Studies Oceanogr., vol. 57, no. 1, pp. 111–126, 2010, doi: 10.1016/j.dsr2.2009.08.010.

[10] P. Fernandes, P. Stevenson, A. Brierley, F. Armstrong, and E. Simmons, "Autonomous underwater vehicles: Future platforms for fisheries acoustics," ICES J. Marine Sci., vol. 60, no. 3, pp. 684–691, 2003. [Online]. Available: https://doi.org/10.1016/S1054-3139(03)00038-9

[11] N. Carter, Autonomous Underwater Vehicles: Technology and Applications. New York, NY, USA: Clanrye Int., 2015.

[12] E. D'Asaro, "Performance of autonomous Lagrangian floats," J. Atmos. Ocean. Technol., vol. 20, no. 6, pp. 896–911, 2003, doi: 10.1175/1520-0426(2003)020<0896:POALF>2.0.CO;2.

[13] S. Le Reste, V. Dutreuil, and X. Andre, "'Deep-Arvor': A new profiling float to extend Argo observations down to 4000 m depth," J. Atmos. Ocean. Technol., vol. 33, no. 5, pp. 1039–1055, 2016. [Online]. Available: http://dx.doi.org/10.1175/JTECH-D-15-0214.1

[14] T. Dickey, E. Itsweire, M. Moline, and M. Perry, "Introduction to the limnology and oceanography special issue on autonomous and Lagrangian platforms and sensors (ALPS)," Limnol. Oceanogr., vol. 53, no. 5, pp. 2057–2061, 2008, doi: 10.4319/lo.2008.53.5_part_2.2057.

[15] E. Berkenpas, B. Henning, C. Shepard, and A. Turchik, "The Driftcam: A buoyancy controlled pelagic camera trap," in Proc. OCEANS - San Diego, 2013, pp. 1–6, doi: 10.23919/OCEANS.2013.6741018

[16] E. Berkenpas et al., "A Buoyancy-Controlled Lagrangian Camera Platform for In Situ Imaging of Marine Organisms in Midwater Scattering Layers," in IEEE Journal of Oceanic Engineering, vol. 43, no. 3, pp. 595-607, July 2018, doi: 10.1109/JOE.2017.2736138.'

[17] T. Fossen, *Handbook of marine craft hydrodynamics and motion control*. John Wiley & Sons, 2011.

[18] R. J. Suitor and D. A. Paley, "Dynamics and control of a buoyancy-driven underwater vehicle for estimating and tracking the scattering layer," in AIAA SciTech, San Diego, CA, 2022, submitted.